ASTRONOMY
AND
ASTROPHYSICS

Estimating physical quantities for an observed galactic microlensing event

M. Dominik

Institut für Physik, Universität Dortmund, D-44221 Dortmund, Germany

arXiv:astro-ph/9701035v2 13 Nov 1997

Abstract. For a given spatial distribution of the lenses and distribution of the transverse velocity of the lens relative to the line-of-sight, a probability distribution for the lens mass for a single observed event is derived. In addition, similar probability distributions are derived for the Einstein radius and the separation of the lens objects and their rotation period for a binary lens. These probability distributions are distinct from the distributions for the lens population, as investigated e.g. by the mass moment method of De Rújula et al. (1991). It is shown that the expectation value for the mass of a certain event as derived in this paper coincides with the estimated average mass of the underlying mass spectrum as found with the mass moment method when only one event is considered. The special cases of a Maxwellian velocity distribution and of a constant velocity are discussed in detail. For a rudimentary model of the Galactic halo, the probability distributions are shown and the relations between the expectation values of the physical quantities and the event timescale are given. For this model it is shown that within a 95.4 %-interval around the expectation value the mass varies by a factor of 800. For the observed events towards the LMC — including the binary lens models for MACHO LMC#1 (Dominik & Hirshfeld 1996) and MACHO LMC#9 (Bennett et al. 1996) — the results are shown explicitly. I discuss what information can be extracted and how additional information from the ongoing microlensing observations influences the results.

Key words: gravitational lensing — dark matter — Stars: low-mass, brown dwarfs — Galaxy: halo — planetary systems

1. Introduction

Some attempts have been made to obtain information about the mass of the lens from observed microlensing events. Unfortunately, the mass cannot be inferred directly. Instead, the only relevant information directly available from a fit of a light curve to the observed data points is the timescale $t_{\rm E}$, and the mass depends on this timescale ($M \propto t_{\rm E}^2$) as well as on the position of the lens and the transverse velocity of the lens relative to the line-of-sight. Since the latter parameters are both not observable (except for extraordinary cases where some ad-

ditional information can be obtained), one can only obtain statistical information on the lens mass assuming distributions of the lens position and the transverse lens velocity. Griest (1991), cited as GRI in the following, argued that the most likely mass distribution is that which yields the best fit to the distribution of timescales of the observed events. De Rújula et al. (1991), cited as RJM in the following, Jetzer & Massó (1994) and Jetzer (1994) have shown that one can extract statistical moments of the lens mass distribution from the moments of the distribution of the timescales.

While these attempts use the distribution of timescales to obtain information about the mass spectrum of the lenses as realized in nature, I will discuss another topic in this paper. For a given observed event, I investigate the probability distributions of the lens mass and other physical quantities like the Einstein radius and the separation and rotation period of the lens objects for a binary lens. These probability distributions give the answer to the question, how probable certain ranges of the considered physical quantity are for the given lens system having produced the event. Note that this question is not answered by applying the methods of GRI or RJM. It is however of special importance for planetary systems. Also note that additional parameters will enter the calculation of the event rate if one considers events which deviate from the point-source-point-mass-lens model. A binary lens will give serious problems for determining the mass spectrum from the timescale distribution since one measures the agglomeration of two objects each from the mass spectrum for one event rather than a single object from the mass spectrum. In contrast to this, the probability distributions presented in this paper also give meaningful results for 'anomalous' events.

This paper is organized as follows. In Sect. 2, it is shown which information directly results from a fit of a galactic microlensing light curve. In Sect. 3, the relation between the event rate and the mass spectrum, the spatial distribution of the lenses, and the distribution of the relative velocity is given. Section 4 shows how the probability distribution for the lens mass can be derived. Section 5 gives results for the moments of further physical quantities and the probability distribution of these quantities around their expectation value. In Sect. 6, it is shown that the expectation value for the mass coincides with the value obtained by applying the mass moment method of

RJM to one event. In Sect. 7, two special forms of the velocity distribution are discussed in more detail: a Maxwellian distribution and a fixed velocity. In Sect. 8, the expectation values and the probability distributions for the lens mass, the Einstein radius, and the separation and the rotation period for binary lenses are shown for a simple model of the galactic halo. In addition, intervals corresponding to probabilites of 68.3 % and 95.4 % are given for these quantities. In Sect. 9, the implications for the observed events towards the LMC (Alcock et al. 1993; Auborg et al. 1993; Dominik & Hirshfeld 1996; Alcock et al. 1996, 1997; Pratt et al. 1996; Bennett et al. 1996) are discussed explicitly. I discuss what information can be extracted and how the observation of more events influences the results.

2. Information from a fit of a galactic microlensing event

From a fit of the light curve to the observed data of a galactic microlensing event, the only dimensional parameters are the point of time t_{max} when the event occurs and the characteristic timescale t_{E} related to its duration. While the point of time t_{max} does not yield any relevant information, all physical quantities related to the observed event which involve a dimension depend on t_{E}. This is true not only for the 'standard model' of Galactic microlensing — a point-mass lens and a point source —, but also for 'anomalous' events (binary sources and lenses, parallax effects, blending, finite size of the source and the lens).[1] The geometry of the microlensing events depends on a length scale which can be chosen as the Einstein radius r_{E} of the lens of mass M at a distance D_{d} from the observer, where the source is at a distance D_{s} from the observer and at a distance D_{ds} from the lens. The Einstein radius r_{E} is then given by

$$r_{\mathrm{E}} = \sqrt{\frac{4GM}{c^2} \frac{D_{\mathrm{d}} D_{\mathrm{ds}}}{D_{\mathrm{s}}}} \,. \tag{1}$$

With $\mu = M/M_{\odot}$ and $x = D_{\mathrm{d}}/D_{\mathrm{s}}$, r_{E} can be written as

$$r_{\mathrm{E}} = r_0 \sqrt{\mu x(1-x)} \tag{2}$$

where

$$r_0 = \sqrt{\frac{4GM_{\odot} D_{\mathrm{s}}}{c^2}} \,. \tag{3}$$

The characteristic time scale t_{E} is given by

$$t_{\mathrm{E}} = \frac{r_{\mathrm{E}}}{v_{\perp}} \,, \tag{4}$$

where $v_{\perp}$ is the transverse velocity of the lens relative to the line-of-sight source-observer. Note that motions of the source and the observer are also absorbed into this quantity.

For a given t_{E}, the mass μ therefore follows as

$$\mu = \frac{t_{\mathrm{E}}^2}{r_0^2} \frac{v_{\perp}^2}{x(1-x)} = \frac{t_{\mathrm{E}}^2 v_{\mathrm{c}}^2}{r_0^2} \frac{\zeta^2}{x(1-x)} \,, \tag{5}$$

[1] Since these 'anomalous' events correspond to a more general model and the point-source-point-mass-lens model is a special case or an approximation, the 'anomalous' events are quite the normal thing!

where v_{c} is a characteristic velocity and $\zeta = v_{\perp}/v_{\mathrm{c}}$. One sees that μ depends on the timescale t_{E} as well as on x and ζ. By assuming distributions of x and ζ (where the distribution of ζ may depend on x), it should in principle be possible to derive a probability distribution for μ. For doing this, I have a look at the event rate in the next section.

3. Event rate and mass spectrum

Consider a coordinate system where the lens is at rest and let the source move on a straight line projected onto the lens plane with velocity $v_{\perp}$. Following Mao & Paczyński (1991), the characteristic width w is then defined as the range of impact parameters for which a microlensing event occurs. Clearly, the width w is proportional to the Einstein radius r_{E}, so that $w = w_0 r_{\mathrm{E}}(x)$. The event rate Γ is given by the product of the area number density of the lenses, the perpendicular velocity and the characteristic width of the considered type of event:

$$\Gamma = n \, v_{\perp} \, w \,. \tag{6}$$

For variable lens position, the area number density of the lenses has to be replaced by an integral of the volume number density n over the line-of-sight direction x. For a general lens population, the number density depends also on the mass μ of the considered objects, so that one gets

$$D_{\mathrm{s}} \int \frac{dn(x,\mu)}{d\mu} \, d\mu \, dx \tag{7}$$

as area number density of the lenses. If the mass spectrum does not depend on x, one can separate the x and μ-dependence by

$$\frac{dn(x,\mu)}{d\mu} = H(x) \frac{dn_0(\mu)}{d\mu} \,, \tag{8}$$

where the function $H(x)$ follows the volume mass density $\rho(x)$ as $\rho(x) = \rho_0 H(x)$, so that $\rho(x) = \rho_0$ at the reference distance where $H(x) = 1$.

The total volume number density of lenses at the reference distance is

$$n_0 = \int \frac{dn_0(\mu)}{d\mu} \, d\mu \,, \tag{9}$$

so that the probability for a mass μ in the interval $[\mu, \mu + d\mu]$ is

$$\omega(\mu) \, d\mu = \frac{1}{n_0} \frac{dn_0(\mu)}{d\mu} \, d\mu \tag{10}$$

which gives the mass spectrum.

With $\widetilde{H}(v_{\perp}) \, dv_{\perp}$ being the probability of finding the perpendicular velocity in the interval $[v_{\perp}, v_{\perp} + dv_{\perp}]$, one obtains for the event rate

$$\Gamma = D_{\mathrm{s}} w_0 \int r_{\mathrm{E}}(x) H(x) v_{\perp} \widetilde{H}(v_{\perp}) \frac{dn_0(\mu)}{d\mu} \, d\mu \, dv_{\perp} \, dx \tag{11}$$

or

$$\Gamma = \frac{D_{\mathrm{s}} w_0}{<M>} \int r_{\mathrm{E}}(x) \rho(x) v_{\perp} \widetilde{H}(v_{\perp}) \, \omega(\mu) \, d\mu \, dv_{\perp} \, dx \tag{12}$$

with the average mass $<M>=\frac{\rho_0}{n_0}$.

Let v_c be a characteristic velocity and $\zeta = \frac{v_\perp}{v_c}$. The probability density for ζ is then given by

$$\widetilde{K}(\zeta) = \widetilde{H}(\zeta v_c)\, v_c\,. \tag{13}$$

Note that $\widetilde{K}$ may depend on x. For any x, $\widetilde{K}$ is normalized as

$$\int \widetilde{K}(\zeta; x)\, d\zeta = 1\,. \tag{14}$$

With these definitions and $r_E^2 = r_0^2 \mu x(1-x)$, one gets

$$\Gamma = D_s w_0\, r_0\, v_c \int \sqrt{\mu x(1-x)}\, H(x)\, \zeta\, \widetilde{K}(\zeta)\, \cdot$$
$$\cdot \frac{dn_0(\mu)}{d\mu}\, d\mu\, d\zeta\, dx\,. \tag{15}$$

4. The probability density for the mass

Eq. (15) gives the total event rate which includes events with all possible timescales from the mass spectrum and the distribution of the lens position and velocity. By adding an integration over t_E and a δ-function one gets

$$\Gamma = D_s w_0\, r_0\, v_c \int \sqrt{\mu x(1-x)}\, H(x)\, \zeta\, \widetilde{K}(\zeta) \frac{dn_0(\mu)}{d\mu}\, \cdot$$
$$\cdot \delta\left(t_E - \frac{r_0}{v_c\, \zeta}\sqrt{\mu x(1-x)}\right) dt_E\, d\mu\, d\zeta\, dx\,. \tag{16}$$

The event rate contribution for timescales t_E in the interval $[t_E, t_E + dt_E]$ is given by $\frac{d\Gamma}{dt_E}\, dt_E$.

Let us now compare different mass spectra which have only the mass μ', i.e.

$$\frac{dn_0}{d\mu}(\mu) \propto \delta(\mu - \mu')\,. \tag{17}$$

If one assigns the same probability to any mass a-priori, one has $\omega(\mu) = \delta(\mu - \mu')$, i.e.

$$\frac{dn_0}{d\mu}(\mu) = \frac{\rho_0}{\mu M_\odot}\, \delta(\mu - \mu')\,. \tag{18}$$

More generally, one can use any explicit form of the mass spectrum, e.g. a power law for $\frac{dn_0}{d\mu}$ by using a weighting factor $\alpha\, \mu^p$, i.e.

$$\frac{dn_0}{d\mu}(\mu) = \alpha\, \mu^p\, \delta(\mu - \mu')\,, \tag{19}$$

so that the case above corresponds to $p = -1$.

For the power-law mass spectra, one obtains

$$\frac{d\Gamma}{dt_E} = D_s w_0\, r_0\, v_c\, \alpha \int \mu'^{p+1/2}\, \sqrt{x(1-x)}\, H(x)\, \cdot$$
$$\cdot \zeta\, \widetilde{K}(\zeta)\, \delta\left(t_E - \frac{r_0}{v_c\, \zeta}\sqrt{\mu' x(1-x)}\right) d\zeta\, dx\,. \tag{20}$$

For a given μ', the probability for a timescale in the interval $[t_E, t_E + dt_E]$ is given by $\frac{1}{\Gamma}\frac{d\Gamma}{dt_E}\, dt_E$ as a function of t_E. This fact has been used by GRI and RJM to compare the distribution

of the timescales t_E for different masses μ'. By exchanging the roles of μ' and t_E one obtains the contribution of masses in the interval $[\mu', \mu' + d\mu']$ for events with t_E to the event rate as (μ' is called μ in the following)

$$\frac{d\Gamma}{d\mu} = D_s w_0 r_0\, v_c\, \alpha \int \mu^{p+1/2}\, \sqrt{x(1-x)}\, H(x)\, \cdot$$
$$\cdot \zeta\, \widetilde{K}(\zeta)\, \delta\left(\mu - \frac{t_E^2 v_c^2 \zeta^2}{r_0^2 x(1-x)}\right) dx\, d\zeta\,, \tag{21}$$

so that $\frac{1}{\Gamma}\frac{d\Gamma}{d\mu}$ gives the probability density for the mass μ.

The normalization factor is obtained by integration over μ, which gives

$$\Gamma = D_s w_0\, t_E^{2p+1}\, v_c^{2p+2}\, r_0^{-2p}\, \alpha\, \cdot$$
$$\cdot \int [x(1-x)]^{-p}\, H(x)\, \zeta^{2p+2}\, \widetilde{K}(\zeta)\, dx\, d\zeta$$
$$= D_s w_0\, t_E^{2p+1}\, v_c^{2p+2}\, r_0^{-2p}\, \alpha\, T(-p, 2p+2)\,, \tag{22}$$

where

$$T(r, s) = \int [x(1-x)]^r\, H(x)\, \zeta^s\, \widetilde{K}(\zeta)\, d\zeta\, dx\,. \tag{23}$$

For the case that the velocity distribution does not depend on x, the function $T(r, s)$ separates as

$$T(r, s) = \Xi(r)\, W(s)\,, \tag{24}$$

where

$$\Xi(r) = \int [x(1-x)]^r\, H(x)\, dx\,, \tag{25}$$

$$W(s) = \int \zeta^s\, \widetilde{K}(\zeta)\, d\zeta\,. \tag{26}$$

The probability density for μ follows as

$$\frac{1}{\Gamma}\frac{d\Gamma}{d\mu} = \frac{1}{T(-p, 2p+2)}\left(\frac{r_0}{t_E\, v_c}\right)^{2p+1} \int \mu^{p+1/2}\, \cdot$$
$$\cdot \sqrt{x(1-x)}\, H(x)\, \zeta\, \widetilde{K}(\zeta)\, \delta\left(\mu - \frac{t_E^2 v_c^2 \zeta^2}{r_0^2 x(1-x)}\right) dx\, d\zeta\,. \tag{27}$$

Note that the width w_0 has cancelled out. This is due to the fact that the fit parameters are kept fixed and only the unknown quantities μ, x, and $v_\perp$ are varied. Implicitly, the same probability is assigned to each parameter for the different values of μ, x, and ζ.

5. Moments of the probability distributions for physical quantities

The expectation value $<\mu>$ follows as

$$<\mu> = \int \frac{1}{\Gamma}\frac{d\Gamma}{d\mu}\, \mu\, d\mu$$
$$= \frac{1}{T(-p, 2p+2)} \int \mu(t_E, x, \zeta)\, [x(1-x)]^{-p}\, H(x)\, \cdot$$
$$\cdot \zeta^{2p+2}\, \widetilde{K}(\zeta)\, d\zeta\, dx\,, \tag{28}$$

and for a general quantity $G = G(t_{\mathrm{E}}, x, \zeta)$ one obtains

$$
\begin{aligned}
<G> &= \int \frac{1}{\Gamma} \frac{d\Gamma}{d\mu} G \, d\mu \\
&= \frac{1}{T(-p, 2p+2)} \int G(t_{\mathrm{E}}, x, \zeta) \left[x(1-x)\right]^{-p} H(x) \cdot \\
&\quad \cdot \zeta^{2p+2} \, \widetilde{K}(\zeta) \, d\zeta \, dx \, .
\end{aligned}
\tag{29}
$$

This means that one averages over x with the density function $[x(1-x)]^{-p} H(x)$ and over ζ with the density function $\zeta^{2p+2} \, \widetilde{K}(\zeta)$.

For the quantity G being of the form

$$
G(t_{\mathrm{E}}, x, \zeta) = G_0(t_{\mathrm{E}}) \left[x(1-x)\right]^k \zeta^l
\tag{30}
$$

one obtains

$$
<G> = G_0 \frac{T(k-p, l+2p+2)}{T(-p, 2p+2)} = G_0 \, F(p, k, l) \, .
\tag{31}
$$

For the mass, one has

$$
\mu(t_{\mathrm{E}}, x, \zeta) = \frac{t_{\mathrm{E}}^2 \, v_{\mathrm{c}}^2}{r_0^2} \frac{\zeta^2}{x(1-x)} \, ,
\tag{32}
$$

so that $k = -1$ and $l = 2$, and

$$
<\mu> = \frac{t_{\mathrm{E}}^2 \, v_{\mathrm{c}}^2}{r_0^2} \frac{T(-1-p, 2p+4)}{T(-p, 2p+2)} \, .
\tag{33}
$$

For $p = -1$, this gives

$$
<\mu> = \frac{t_{\mathrm{E}}^2 \, v_{\mathrm{c}}^2}{r_0^2} \frac{T(0, 2)}{\Xi(1)} \, ,
\tag{34}
$$

which is the same value as for the average mass in the mass spectrum (if one uses only the information from a single event), which can obtained by the method of mass moments described in Sect. 6. Note however that the probability density for μ for a specific event and the mass spectrum are different quantities and that the higher moments are different.

If the velocity distribution does not depend on x, one gets for the expectation value of the mass

$$
<\mu> = \frac{t_{\mathrm{E}}^2 \, v_{\mathrm{c}}^2}{r_0^2} \frac{\Xi(0) \, W(2)}{\Xi(1)} \, .
\tag{35}
$$

$\Xi(0)$ is related to the surface mass density Σ by

$$
\Sigma = \int_0^{D_{\mathrm{s}}} \rho(D_{\mathrm{d}}) \, dD_{\mathrm{d}} = D_{\mathrm{s}} \rho_0 \int_0^1 H(x) \, dx = D_{\mathrm{s}} \rho_0 \, \Xi(0) \, ,
\tag{36}
$$

and $\Xi(1)$ is related to the optical depth τ by

$$
\begin{aligned}
\tau &= \int_0^{D_{\mathrm{s}}} \frac{4\pi G D}{c^2} \, \rho(D_{\mathrm{d}}) \, dD_{\mathrm{d}} \\
&= \frac{4G}{c^2} \, D_{\mathrm{s}}^2 \, \rho_0 \, \pi \int_0^1 H(x) x(1-x) \, dx \\
&= r_0^2 \frac{D_{\mathrm{s}} \rho_0}{M_\odot} \pi \, \Xi(1) \, .
\end{aligned}
\tag{37}
$$

Using these results, and noting that

$$
<v_\perp^2> = v_{\mathrm{c}}^2 \, W(2) \, ,
\tag{38}
$$

the expectation value of the mass can be written in the convenient form

$$
<\mu> = t_{\mathrm{E}}^2 \, v_{\mathrm{c}}^2 \, W(2) \frac{\pi}{\tau} \frac{\Sigma}{M_\odot}
\tag{39}
$$

using the optical depth τ, the area number density of the lenses Σ, the average square of the velocity $<v_\perp^2>$, and the timescale t_{E}. Note that $<\mu>$ depends only on $<v_\perp^2>$, not on the form of the velocity distribution.

To investigate the distribution of G around $<G>$, I define

$$
\kappa_G = \frac{G}{<G>} = \frac{[x(1-x)]^k \zeta^l}{F(p, k, l)} \, .
\tag{40}
$$

Using

$$
\widetilde{\mu}(t_{\mathrm{E}}, x, \zeta) = \mu \frac{r_0^2}{t_{\mathrm{E}}^2 v_{\mathrm{c}}^2} = \frac{\zeta^2}{x(1-x)} \, ,
\tag{41}
$$

one obtains for κ_G the probability density

$$
\begin{aligned}
p(\kappa_G) &= \frac{1}{\Gamma} \frac{d\Gamma}{d\kappa_G} \\
&= \frac{1}{T(-p, 2p+2)} \left(\frac{r_0}{t_{\mathrm{E}} v_{\mathrm{c}}}\right)^{2p+1} \int [\mu(\kappa_G)]^{p+1/2} \cdot \\
&\quad \cdot \sqrt{x(1-x)} \, H(x) \, \zeta \, \widetilde{K}(\zeta) \cdot \\
&\quad \cdot \delta\left(\kappa_G - \kappa_G(x, \zeta)\right) \, dx \, d\zeta \\
&= \frac{1}{T(-p, 2p+2)} \int [\widetilde{\mu}(\kappa_G)]^{p+1/2} \, \sqrt{x(1-x)} \cdot \\
&\quad \cdot H(x) \, \zeta \, \widetilde{K}(\zeta) \cdot \\
&\quad \cdot \delta\left(\kappa_G - \frac{[x(1-x)]^k \zeta^l}{F(p, k, l)}\right) \, dx \, d\zeta \\
&= \frac{F(p, k, l)}{T(-p, 2p+2)} \frac{1}{|l|} \int [\widetilde{\mu}(\kappa_G)]^{p+1/2} \cdot \\
&\quad \cdot [x(1-x)]^{1/2-k} \, H(x) \, \zeta^{-l+2} \, \widetilde{K}(\zeta) \cdot \\
&\quad \cdot \delta\left(\frac{\kappa_G F(p, k, l)}{[x(1-x)]^k} - \zeta^l\right) \, dx \, d(\zeta^l) \\
&= \frac{[F(p, k, l)]^{\frac{2p+3}{l}}}{|l| \, T(-p, 2p+2)} \kappa_G^{\frac{2p-l+3}{l}} \cdot \\
&\quad \cdot \int [x(1-x)]^{-p-(3+2p)\frac{k}{l}} \, H(x) \cdot \\
&\quad \cdot \widetilde{K}\left(\left(\frac{\kappa_G F(p, k, l)}{[x(1-x)]^k}\right)^{1/l}\right) \, dx \, .
\end{aligned}
\tag{42}
$$

Note that this distribution depends only on the form of the distributions of x and ζ and not on any physical parameters like v_{c} or ρ_0.

The distribution of $\lambda_G = \lg \kappa_G$ is given by

$$
\psi(\lambda_G) = \frac{\ln 10 \cdot \left[F(k, p, l) \cdot 10^{\lambda_G}\right]^{\frac{2p+3}{l}}}{|l| \, T(-p, 2p+2)} \, .
$$

$$\cdot \int [x(1-x)]^{-p-(3+2p)\frac{k}{l}} H(x) \cdot$$

$$\cdot \widetilde{K}\left(\left(\frac{10^{\lambda_G}}{[x(1-x)]^k} F(p,k,l)\right)^{1/l}\right) dx. \qquad (43)$$

All moments of the probability distribution of G can be reduced to the function $T(k,j)$, which separates as the product of $\Xi(k)$ and $W(j)$ if the velocity distribution does not depend on x. For the n-th moment one has

$$<G^n> = \int \frac{1}{\Gamma} \frac{d\Gamma}{d\mu} G^n d\mu = G_0^n F(p,nk,nl). \qquad (44)$$

The relative deviation of G is given by

$$\sigma_{\kappa_G} = \frac{\sigma_G}{<G>} = \frac{\sqrt{<G^2> - <G>^2}}{<G>} = \sqrt{\frac{<G^2>}{<G>^2} - 1}. \qquad (45)$$

With

$$\begin{aligned} F_2(p,k,l) &= \frac{F(p,2k,2l)}{[F(p,k,l)]^2} \\ &= \frac{T(2k-p, 2l+2p+2)}{[T(k-p, l+2p+2)]^2} T(-p, 2p+2), \quad (46) \end{aligned}$$

one obtains

$$\sigma_{\kappa_G} = \frac{\sigma_G}{<G>} = \sqrt{F_2(p,k,l) - 1}. \qquad (47)$$

6. The method of mass moments

For the moments of the t_E-distribution for several events, one obtains following RJM

$$\begin{aligned} \overline{t_E^m} &= \frac{1}{\Gamma} \int \frac{d\Gamma}{dt_E} t_E^m dt_E \\ &= \frac{D_s w_0 r_0 v_c}{\Gamma} \int \sqrt{\mu x(1-x)} H(x) \zeta \widetilde{K}(\zeta) \frac{dn_0(\mu)}{d\mu} \cdot \\ &\quad \cdot t_E^m \delta\left(t_E - \frac{r_0}{v_c \zeta}\sqrt{\mu x(1-x)}\right) dt_E d\mu d\zeta dx \\ &= \frac{D_s w_0 r_0^{m+1} v_c^{1-m}}{\Gamma} \int \mu^{\frac{m+1}{2}} \frac{dn_0(\mu)}{d\mu} d\mu \cdot \\ &\quad \cdot \int [x(1-x)]^{\frac{m+1}{2}} H(x) \zeta^{1-m} \widetilde{K}(\zeta) d\zeta dx \\ &= \frac{D_s w_0 r_0^{m+1} v_c^{1-m}}{\Gamma} n_0 \overline{\mu^{\frac{m+1}{2}}} T\left(\frac{m+1}{2}, 1-m\right), (48) \end{aligned}$$

where

$$\overline{\mu^k} = \frac{1}{n_0} \int \mu^k \frac{dn_0(\mu)}{d\mu} d\mu = \int \mu^k \omega(\mu) d\mu. \qquad (49)$$

$\overline{\mu^k}$ yields for the case $k=0$, $\overline{\mu^0} = 1$, and for $k=1$ the average mass (in units of $M_\odot$) as

$$\overline{\mu} = \int \mu \omega(\mu) d\mu = \frac{1}{n_0} \int \frac{dn_0(\mu)}{d\mu} \mu d\mu = \frac{\rho_0}{n_0 M_\odot}. \qquad (50)$$

One sees that the moments of the mass spectrum can be extracted from the moments of the time-scale distribution if the spatial distribution of the mass density and the velocity distribution is given (RJM).

For the moments of the mass spectrum one gets

$$\overline{\mu^k} = \frac{\Gamma}{D_s w_0 n_0} \frac{v_c^{2k-2}}{r_0^{2k}} \frac{1}{T(k, 2-2k)} \overline{t_E^{2k-1}}. \qquad (51)$$

This gives for $k=0$

$$1 = \overline{\mu^0} = \frac{\Gamma}{D_s w_0 n_0 v_c^2} \frac{1}{T(0,2)} \overline{t_E^{-1}}, \qquad (52)$$

which yields

$$n_0 = \frac{\Gamma}{D_s w_0 v_c^2} \frac{1}{T(0,2)} \overline{t_E^{-1}}, \qquad (53)$$

so that

$$\overline{\mu^k} = \frac{v_c^{2k}}{r_0^{2k}} \frac{T(0,2)}{T(k, 2-2k)} \frac{\overline{t_E^{2k-1}}}{\overline{t_E^{-1}}}. \qquad (54)$$

For $k=1$, one obtains

$$\overline{\mu} = \frac{\overline{t_E}}{\overline{t_E^{-1}}} \frac{v_c^2}{r_0^2} \frac{T(0,2)}{T(1,0)} = \frac{\overline{t_E}}{\overline{t_E^{-1}}} \frac{v_c^2}{r_0^2} \frac{T(0,2)}{\Xi(1)}, \qquad (55)$$

since $T(1,0) = \Xi(1)$, which is the same value as obtained for the expectation value of the lens mass for $p = -1$ as derived above, if one considers a single observed event.

7. Special forms of the velocity distribution $\widetilde{K}(\zeta)$

7.1. Maxwell distribution

A distribution

$$\widetilde{H}(v_\perp) = \frac{2v_\perp}{v_c^2} \exp\left\{-\frac{v_\perp^2}{v_c^2}\right\} \qquad (56)$$

implies

$$\widetilde{K}(\zeta) = 2\zeta \exp\left\{-\zeta^2\right\}, \qquad (57)$$

and for $p(\kappa_G)$ and $\psi(\lambda_G)$ one has from Eqs. (42) and (43)

$$\begin{aligned} p(\kappa_G) &= \frac{2[F(p,k,l)]^{\frac{2p+4}{l}}}{|l| \Xi(-p) W(2p+2)} \kappa_G^{\frac{2p+4}{l}-1} \cdot \\ &\quad \cdot \int [x(1-x)]^{-p-(4+2p)\frac{k}{l}} H(x) \cdot \\ &\quad \cdot \exp\left\{-\left(\frac{\kappa_G F(p,k,l)}{[x(1-x)]^k}\right)^{2/l}\right\} dx, \qquad (58) \end{aligned}$$

$$\begin{aligned} \psi(\lambda_G) &= \frac{2\ln 10 \cdot \left[F(k,p,l) \cdot 10^{\lambda_G}\right]^{\frac{2p+4}{l}}}{|l| \Xi(-p) W(2p+2)} \cdot \\ &\quad \cdot \int [x(1-x)]^{-p-(4+2p)\frac{k}{l}} H(x) \cdot \\ &\quad \cdot \exp\left\{-\left(\frac{10^{\lambda_G}}{[x(1-x)]^k} F(p,k,l)\right)^{2/l}\right\} dx. \qquad (59) \end{aligned}$$

For $p = -1$ and separation of the spatial distribution and velocity distribution, these equations read

$$p(\kappa_G) = \frac{2}{|l| \,\Xi(1)} \left(\frac{\Xi(k+1)W(l)}{\Xi(1)}\right)^{2/l} \kappa_G^{\frac{2}{l}-1} \cdot$$
$$\cdot \int [x(1-x)]^{1-2\frac{k}{l}} H(x) \cdot$$
$$\cdot \exp\left\{-\left(\frac{\kappa_G}{[x(1-x)]^k}\, \frac{\Xi(k+1)W(l)}{\Xi(1)}\right)^{2/l}\right\} dx, \quad (60)$$

$$\psi(\lambda_G) = \frac{2\ln 10 \cdot 10^{\frac{2\lambda_G}{l}}}{l|\,\Xi(1)} \left(\frac{\Xi(k+1)W(l)}{\Xi(1)}\right)^{2/l} \cdot$$
$$\cdot \int [x(1-x)]^{1-2\frac{k}{l}} H(x) \cdot$$
$$\cdot \exp\left\{-\left(\frac{10^{\lambda_G}}{[x(1-x)]^k}\, \frac{\Xi(k+1)W(l)}{\Xi(1)}\right)^{2/l}\right\} dx. \quad (61)$$

Examples for these distributions are shown in Sect. 8, where the galactic halo is discussed.

7.2. Fixed velocity

A model with a fixed velocity corresponds to

$$\widetilde{K}(\zeta) = \delta(\zeta - 1). \quad (62)$$

It follows that $W(n) = 1 \;\forall n$ and $F(p,k,l)$ does not depend on l, so that

$$F(p,k,l) = \Phi(p,k) \quad (63)$$

with

$$\Phi(p,k) = \frac{\Xi(k-p)}{\Xi(-p)}. \quad (64)$$

With Eq. (42), $p(\kappa_G)$ follows as

$$p(\kappa_G) = \frac{[\Phi(p,k)]^{\frac{2p+3}{l}}}{|l| \,\Xi(-p)} \kappa_G^{\frac{2p+3}{l}-1} \int [x(1-x)]^{-p-(3+2p)\frac{k}{l}} \cdot$$
$$\cdot H(x)\,\delta\left(\left(\frac{\kappa_G\,\Phi(p,k)}{[x(1-x)]^k}\right)^{1/l} - 1\right) dx$$
$$= \frac{[\Phi(p,k)]^{\frac{2p+3}{l}}}{|l| \,\Xi(-p)} \kappa_G^{\frac{2p+3}{l}-1} \int [x(1-x)]^{-p-(2+2p)\frac{k}{l}} \cdot$$
$$\cdot H(x) \cdot$$
$$\cdot \delta\left((\kappa_G\,\Phi(p,k))^{1/l} - [x(1-x)]^{k/l}\right) dx. \quad (65)$$

With the substitution

$$d[x(1-x)]^{k/l} = \frac{k}{l}\,[x(1-x)]^{k/l-1}(1-2x)\,dx, \quad (66)$$

one gets

$$p(\kappa_G) = \frac{[\Phi(p,k)]^{\frac{2p+3}{l}}}{|k| \,\Xi(-p)} \kappa_G^{\frac{2p+3}{l}-1}.$$

$$\cdot \int [x(1-x)]^{-p+1-(3+2p)\frac{k}{l}} \left|\frac{1}{1-2x}\right| H(x) \cdot$$
$$\cdot \delta\left((\kappa_G\,\Phi(p,k))^{1/l} - [x(1-x)]^{k/l}\right) \cdot$$
$$\cdot d\left([x(1-x)]^{k/l}\right). \quad (67)$$

The argument of the δ-function is zero for

$$x = \frac{1}{2}\left(1 \pm \sqrt{1 - 4\,(\kappa_G\,\Phi(p,k))^{1/k}}\right), \quad (68)$$

so that

$$1 - 2x = \mp\sqrt{1 - 4\,(\kappa_G\,\Phi(p,k))^{1/k}}. \quad (69)$$

This yields for $p(\kappa_G)$

$$p(\kappa_G) = \frac{[\Phi(p,k)]^{\frac{1-p}{k}}}{|k| \,\Xi(-p)} \kappa_G^{\frac{1-p}{k}-1}\, \frac{1}{\sqrt{1 - 4\,(\kappa_G\,\Phi(p,k))^{1/k}}} \cdot$$
$$\cdot \left[H\left(\frac{1}{2}\left(1 + \sqrt{1 - 4\,(\kappa_G\,\Phi(p,k))^{1/k}}\right)\right) + \right.$$
$$\left. + H\left(\frac{1}{2}\left(1 - \sqrt{1 - 4\,(\kappa_G\,\Phi(p,k))^{1/k}}\right)\right) \right]. \quad (70)$$

Note that $p(\kappa_G)$ does not depend on l.

Since there exist (real) solutions for x only for

$$[\kappa_G\,\Phi(p,k)]^{1/k} \le \frac{1}{4}, \quad (71)$$

κ_G is restricted by $\kappa_G \le \kappa_{G,\mathrm{crit}}$ for $k > 0$, or by $\kappa_G \ge \kappa_{G,\mathrm{crit}}$ for $k < 0$, where

$$\kappa_{G,\mathrm{crit}} = \frac{1}{4^k\,\Phi(p,k)}. \quad (72)$$

Since $<G> = G_0\,\Phi(p,k)$, the critical value of G is

$$G_\mathrm{crit} = \kappa_{G,\mathrm{crit}}\, <G> = \frac{G_0}{4^k}, \quad (73)$$

which is a maximum for $k > 0$ and a minimum for $k < 0$.

The distribution of G can be written in terms of

$$\widetilde{\kappa_G} = \frac{G}{G_\mathrm{crit}} = \frac{\kappa_G}{\kappa_{G,\mathrm{crit}}} = \kappa_G\,4^k\,\Phi(p,k), \quad (74)$$

which yields the probability density

$$\widetilde{p}(\widetilde{\kappa_G}) = \frac{1}{4^{1-p}|k|\,\Xi(-p)} \widetilde{\kappa_G}^{\frac{1-p}{k}-1}\, \frac{1}{\sqrt{1 - \widetilde{\kappa_G}^{1/k}}} \cdot \quad (75)$$
$$\cdot \left[H\left(\frac{1}{2}\left(1 + \sqrt{1 - \widetilde{\kappa_G}^{1/k}}\right)\right) + \right.$$
$$\left. + H\left(\frac{1}{2}\left(1 - \sqrt{1 - \widetilde{\kappa_G}^{1/k}}\right)\right) \right], \quad (76)$$

and for $\widetilde{\lambda_G} = \lg\widetilde{\kappa_G}$ one gets the probability density

$$\widetilde{\psi}(\widetilde{\lambda_G}) = \frac{\ln 10}{4^{1-p}|k|\,\Xi(-p)} 10^{\widetilde{\lambda_G}\frac{1-p}{k}}\, \frac{1}{\sqrt{1 - 10^{\widetilde{\lambda_G}/k}}} \cdot \quad (77)$$
$$\cdot \left[H\left(\frac{1}{2}\left(1 + \sqrt{1 - 10^{\widetilde{\lambda_G}/k}}\right)\right) + \right.$$
$$\left. + H\left(\frac{1}{2}\left(1 - \sqrt{1 - 10^{\widetilde{\lambda_G}/k}}\right)\right) \right], \quad (78)$$

Since

$$
\begin{aligned}
\lambda_G &= \lg \kappa_G = \lg \left(\widetilde{\kappa_G}\, \kappa_{G,\mathrm{crit}} \right) \\
&= \widetilde{\lambda_G} - \lg \Phi(p,k) - 2k \lg 2 \,,
\end{aligned}
\tag{79}
$$

$\psi(\lambda_G)$ is given by

$$
\psi(\lambda_G) = \widetilde{\psi}(\lambda_G + \lg \Phi(p,k) + 2k \lg 2) \,.
\tag{80}
$$

8. Estimates and probability distributions for physical quantities for a simple galactic halo model

The quantities to be discussed here are

- the transverse velocity $v_\perp$,
- the Einstein radius r_E (which immediately yields the projected distance $2\chi r_\mathrm{E}$),
- the mass $M = \mu M_\odot$,
- the rotation period T of a binary.

For these quantities, $G(t_\mathrm{E}, x, \zeta)$, k, l, and $F(-1,k,l)$ ares shown in Table 1. The right expression for $F(-1,k,l)$ is valid if the velocity distribution does not depend on x, ρ denotes the semimajor axis in units of Einstein radii.

For the galactic halo, a velocity distribution of

$$
\widetilde{H}(v_\perp) = \frac{2v_\perp}{v_c^2} \exp\left\{ -\frac{v_\perp^2}{v_c^2} \right\}
\tag{81}
$$

can be used, where $\overline{v_\perp^2} = v_c^2$.

The mass density of halo objects is modelled as

$$
\rho(r) = \rho_0 \frac{a^2 + R_{\mathrm{GC}}^2}{a^2 + r^2} \,,
\tag{82}
$$

where r measures the distance from the Galactic center, R_{GC} is the distance from the sun to the Galactic center, a is a characteristic core radius and ρ_0 is the local density at the position of the sun.

With the distance parameter x, which measures the distance along the line-of-sight from the observer to the LMC in units of the total distance D_s, one obtains

$$
\rho(x) = \rho_0 \frac{1 + \frac{a^2}{R_{\mathrm{GC}}^2}}{1 + \frac{a^2}{R_{\mathrm{GC}}^2} + x^2 \frac{D_\mathrm{s}^2}{R_{\mathrm{GC}}^2} - 2x \frac{D_\mathrm{s}}{R_{\mathrm{GC}}} \cos\alpha} \,,
\tag{83}
$$

where α is the angle between direction of the Galactic center and the direction of the LMC measured from the observer.

With

$$
\xi_\mathrm{s} = \frac{D_\mathrm{s}}{R_{\mathrm{GC}}} \,, \quad A = 1 + \frac{a^2}{R_{\mathrm{GC}}^2} \,, \quad B = -2\cos\alpha \,,
\tag{84}
$$

H(x) can be written as

$$
H(x) = \frac{A}{A + Bx\xi_\mathrm{s} + x^2\xi_\mathrm{s}^2} \,.
\tag{85}
$$

Let the halo be extended to a distance of D_h along the line-of-sight. With $\xi_h = D_\mathrm{h}/R_{\mathrm{GC}}$ and $\xi = \xi_\mathrm{h}/\xi_\mathrm{s}$, one obtains

$$
\begin{aligned}
\Xi(0) &= \int_0^\xi H(x)\, dx \\
&= \int_0^\xi \frac{A}{A + Bx\xi_\mathrm{s} + x^2\xi_\mathrm{s}^2}\, dx \\
&= \frac{A}{\xi_\mathrm{s}} \int_0^{\xi_\mathrm{h}} \frac{1}{A + B\widetilde{x} + \widetilde{x}^2}\, d\widetilde{x} \\
&= \frac{A}{\xi_\mathrm{s}} \frac{2}{\sqrt{4A - B^2}} \left[\arctan\frac{2\xi_\mathrm{h} + B}{\sqrt{4A - B^2}} - \right. \\
&\qquad \left. - \arctan\frac{B}{\sqrt{4A - B^2}} \right] \,,
\end{aligned}
\tag{86}
$$

and

$$
\begin{aligned}
\Xi(1) &= \int_0^\xi x(1-x)\, H(x)\, dx \\
&= A \int_0^\xi \frac{x(1-x)}{A + Bx\xi_\mathrm{s} + x^2\xi_\mathrm{s}^2}\, dx \\
&= \frac{A}{\xi_\mathrm{s}^3} \int_0^{\xi_\mathrm{h}} \frac{\widetilde{x}(\xi_\mathrm{s} - \widetilde{x})}{A + B\widetilde{x} + \widetilde{x}^2}\, d\widetilde{x} \\
&= \frac{A}{\xi_\mathrm{s}^3} \left\{ -\xi_\mathrm{h} + \frac{1}{2}(\xi_\mathrm{s} + B) \ln\frac{A + B\xi_\mathrm{h} + \xi_\mathrm{h}^2}{A} - \right. \\
&\qquad - \frac{\xi_\mathrm{s}B + B^2 - 2A}{\sqrt{4A - B^2}} \left[\arctan\frac{2\xi_\mathrm{h} + B}{\sqrt{4A - B^2}} - \right. \\
&\qquad \left. \left. - \arctan\frac{B}{\sqrt{4A - B^2}} \right] \right\} \,.
\end{aligned}
\tag{87}
$$

Other values of $\Xi(r)$ can be obtained numerically.

Selected values for $\Xi(r)$ and $W(s)$ and $F(-1,k,l)$ are shown in Tables 2, 3, and 4, using the values used by Paczyński (1986)[2]

$$
\begin{aligned}
D_\mathrm{s} &= 50 \text{ kpc} \,, \quad R_{\mathrm{GC}} = 10 \text{ kpc} \,, \quad x_\mathrm{s} = 5 \,, \quad x_\mathrm{h} = 5 \,, \\
&\qquad\qquad \alpha = 82° \,, \quad a = 0 \,.
\end{aligned}
$$

From these values, one obtains for the expectation values:

$$
<v_\perp> = \frac{1}{2}\sqrt{\pi}\, v_\mathrm{c} = 0.886\, v_\mathrm{c} \,,
\tag{88}
$$

$$
<r_\mathrm{E}> = 0.107 \left(\frac{v_\mathrm{c}}{210 \text{ km/s}} \right) \left(\frac{t_\mathrm{E}}{1 \text{ d}} \right) \text{ AU} \,,
\tag{89}
$$

$$
<\mu> = 2.71 \cdot 10^{-4} \left(\frac{v_\mathrm{c}}{210 \text{ km/s}} \right)^2 \left(\frac{t_\mathrm{E}}{1 \text{ d}} \right)^2 \,,
\tag{90}
$$

[2] Using slightly different values for D_s and R_{GC}, and varying the core radius a between 0 and 8 kpc yields estimates which differ by about 5 %.

Table 1. $G(t_E, x, \zeta)$, k, l, and $F(-1, k, l)$ for $v_\perp$, r_E, μ, T

G	$G(t_E, x, \zeta)$	k	l	$F(-1, k, l)$
$v_\perp$	$v_c \zeta$	0	1	$\frac{T(1,1)}{\Xi(1)} = W(1)$
r_E	$t_E v_c \zeta$	0	1	$\frac{T(1,1)}{\Xi(1)} = W(1)$
μ	$\frac{t_E^2 v_c^2}{r_0^2} \frac{\zeta^2}{x(1-x)}$	-1	2	$\frac{T(0,2)}{\Xi(1)} = \frac{\Xi(0)W(2)}{\Xi(1)}$
T	$\frac{4\pi}{c} \sqrt{\rho^3 \, t_E \, D_s \, v_c} \sqrt{x(1-x)} \sqrt{\zeta}$	$\frac{1}{2}$	$\frac{1}{2}$	$\frac{T(\frac{3}{2}, \frac{1}{2})}{\Xi(1)} = \frac{\Xi(\frac{3}{2})W(\frac{1}{2})}{\Xi(1)}$

Table 2. Selected values for $\Xi(r)$

r	$\Xi(r)$
0	0.305
$\frac{1}{2}$	0.105
1	0.0407
$\frac{3}{2}$	0.0168
2	0.00721

Table 3. Selected values for $W(s)$

s	$W(s)$
$-\frac{1}{2}$	1.225
0	1.000
$\frac{1}{2}$	0.906
1	0.886
$\frac{3}{2}$	0.919
2	1.000

Table 4. $F(-1, k, l)$ for $v_\perp$, r_E, μ, T

G	$F(-1, k, l)$
$v_\perp, r_E$	0.886
μ	7.49
T	0.374

$$<T> = 2.63 \, \rho^{3/2} \left(\frac{v_c}{210 \text{ km/s}} \right)^{1/2} \left(\frac{t_E}{1 \text{ d}} \right)^{1/2} \text{a} . \quad (91)$$

With $\rho_0 = \frac{v_c^2}{4\pi G R_{GC}^2}$ one obtains

$$\rho_0 = 8.16 \cdot 10^{-3} \left(\frac{v_c}{210 \text{ km/s}} \right)^2 \frac{M_\odot}{\text{pc}^3} , \quad (92)$$

so that for $v_c = 210$ km/s, one gets $\Sigma = 124 \, M_\odot/\text{pc}^2$ and $\tau = 5 \cdot 10^{-7}$.

The distribution of $\kappa_\mu = \mu/<\mu>$ is given by

$$p(\kappa_\mu) = \frac{\Xi(0)}{(\Xi(1))^2} \int x^2 (1-x)^2 \, H(x) \cdot$$

$$\cdot \exp \left\{ -\frac{\Xi(0)}{\Xi(1)} \kappa_\mu x(1-x) \right\} dx . \quad (93)$$

and the probability density $\psi(\lambda_\mu)$ is

$$\psi(\lambda_\mu) = \frac{\Xi(0)}{(\Xi(1))^2} 10^{\lambda_\mu} \ln 10 \int x^2 (1-x)^2 \, H(x) \cdot$$

$$\cdot \exp \left\{ -\frac{\Xi(0)}{\Xi(1)} 10^{\lambda_\mu} x(1-x) \right\} dx . \quad (94)$$

From Eq. (93) the probability density $P(\mu)$ for the mass μ (in units of $M_\odot$) follows as

$$P(\mu) = \frac{r_0^2}{t_E^2 v_c^2} \frac{1}{\Xi(1)} \int x^2 (1-x)^2 \, H(x) \cdot$$

$$\cdot \exp \left\{ -\frac{\mu \, r_0^2 \, x(1-x)}{t_E^2 v_c^2} \right\} dx , \quad (95)$$

which differs from the probability given by Jetzer & Massó (1994, Eq. (8)), by a factor μ^2/t_E^2. Note that this probability density has to be of the form

$$P(\mu) = \frac{1}{t_E^2} f \left(\frac{\mu}{t_E^2} \right) , \quad (96)$$

since $\mu \propto t_E^2$, to ensure normalization for any t_E.

For the other quantities estimated the probability densities are given by Eqs. (60) and (61). The probability densities $p(\kappa_G)$ and $\psi(\lambda_G)$ for r_E, μ, T are shown in Figs. 1 to 3. Note that r_E follows the velocity distribution, because $k = 0$. In the diagrams for $\psi(\lambda_G)$, symmetric intervals around $<G>$ are shown which give a probability of 68.3 % and 95.4 % respectively. The bounds of these intervals are also shown in Table 5.

The bounds are much larger for r_E and again much larger for μ than for T, which is due to the wide distribution of the velocity and $\mu \propto \zeta^2$, $r_E \propto \zeta$, while $T \propto \sqrt{\zeta}$. The smallest and the largest value in the 95.4 %-interval differ by a factor of about 800 for μ, 16 for r_E and 5 for T.

9. Application to observed events

In this section I show the application of the method described here to the observed events towards the LMC. The first events have been claimed by EROS (Aubourg et al. 1993), namely EROS#1 and #2, and MACHO (Alcock et al. 1993), namely MACHO LMC#1, in 1993. The fit with a point-mass lens and point source for MACHO LMC#1 showed a discrepancy near

Table 5. The bounds of symmetric intervals on a logarithmic scale around $<G>$ which correspond to probabilities of 68.3 % and 95.4 %

G	$\Delta\lambda_{68.3}$	$\Delta\lambda_{95.4}$	$10^{-\Delta\lambda_{68.3}}$	$10^{\Delta\lambda_{68.3}}$	$10^{-\Delta\lambda_{95.4}}$	$10^{\Delta\lambda_{95.4}}$
$v_\perp, r_{\mathrm{E}}$	0.2428	0.6111	0.572	1.75	0.244	4.09
μ	0.5900	1.454	0.257	3.89	0.0351	28.5
T	0.1588	0.3719	0.694	1.44	0.425	2.35

Fig. 1. The probability density $p(\kappa_{v_\perp}) = p(\kappa_{r_{\mathrm{E}}})$ for $\kappa_{v_\perp} = v_\perp/ <v_\perp> = r_{\mathrm{E}}/ <r_{\mathrm{E}}> = \kappa_{r_{\mathrm{E}}}$ (left) and The probability density $\psi(\lambda_{v_\perp}) = \psi(\lambda_{r_{\mathrm{E}}})$ with symmetric 68.3 % and 95.4 % intervals around $<v_\perp>$ or $<r_{\mathrm{E}}>$ (right)

Fig. 2. The probability density $p(\kappa_\mu)$ for $\kappa_\mu = \mu/ <\mu>$ (left) and the probability density $\psi(\lambda_\mu)$ with symmetric 68.3 % and 95.4 % intervals around $<\mu>$ (right)

the peak which has been solved with models involving a binary lens by Dominik & Hirshfeld (1994, 1996). The MACHO collaboration had found two other candidates, MACHO LMC#2 and #3, (Alcock et al. 1996) which have been meanwhile dismissed. In addition, they have claimed the existence of 7 additional events, MACHO LMC#4 to #10, (Pratt et al. 1996),

where MACHO LMC#9 is due to a binary lens (Bennett et al. 1996). In the MACHO data taken from 1996 to March 1997, 5 additional LMC candidates showed up (Stubbs et al. 1997).

It has been shown that the EROS#2 event involves a periodic variable star (Ansari et al. 1995) and that EROS#1 involves an emission line Be type star (Beaulieu et al. 1995), so

Fig. 3. The probability density $p(\kappa_T)$ for $\kappa_T = T/ <T>$ (left) and the probability density $\psi(\lambda_T)$ with symmetric 68.3 % and 95.4 % intervals around $<T>$ (right)

that both EROS#1 and EROS#2 involve a rare type of stars which makes these events suspect as microlensing candidates (e.g. Paczyński 1996). In addition, the MACHO LMC#10 event is likely to be a binary star (Pratt et al. 1996; Alcock et al. 1997).

By assuming that the lens is in the galactic halo and using the halo model of the last section, expectation values for the desired quantities can be obtained by inserting the fit parameters into Eqs. (88) to (91). Table 6 shows the expectation values for the Einstein radius and the mass for the events EROS#1 and EROS#2, MACHO LMC#4...#8 and #10, whereas the results for the binary lens events MACHO LMC#1 and MACHO LMC#9 are shown in Table 7. For MACHO LMC#1 six different binary lens models are shown (Dominik & Hirshfeld 1996; Dominik 1996). Note that the lens for MACHO LMC#9 probably resides in the LMC (Bennett et al. 1996).

The parametrization used is that of Dominik & Hirshfeld (1996): r_{hd} denotes the projected half-distance between the lens objects in the lens plane, where $r_{hd} = 2\chi r_E$, m_1 denotes the mass fraction in lens object 1. $r_E^{(2)}$ denotes the Einstein radius corresponding to the mass of object 2 and $t_E^{(2)}$ the characteristic time corresponding to $r_E^{(2)}$:

$$r_E^{(2)} = r_E \sqrt{1 - m_1}, \tag{97}$$
$$t_E^{(2)} = t_E \sqrt{1 - m_1}. \tag{98}$$

Similarly $\chi^{(1)}$ denotes the projected half-separation in units of Einstein radii corresponding to the mass of object 1, so that

$$\chi^{(1)} = \frac{1}{\sqrt{m_1}} \chi. \tag{99}$$

μ_1 and μ_2 denote the mass in units of $M_\odot$ for objects 1 and 2 and the mass ratio r is given by

$$r = \frac{1 - m_1}{m_1}. \tag{100}$$

Table 8. MACHO LMC#1: Estimates of physical parameters of the binary lens models using a mass ratio r at the upper 2-σ-bound of r and corresponding values of $t_E^{(2)}$ and $\chi^{(1)}$.

	BA	BA1	BA2	BA3
t_E/d	57.67	86.93	29.94	228.6
$t_E^{(2)}$/d	17.63	15.20	17.61	16.49
r	0.1031	0.0315	0.529	0.00523
χ	2.291	2.229	1.735	2.222
$\chi^{(1)}$	2.406	2.264	2.146	2.228
$<r_E>$ /AU	6.20	9.34	3.22	24.6
$<r_E^{(2)}>$ /AU	1.90	1.63	1.89	1.77
$<2r_{hd}>$ /AU	28.4	41.7	11.2	109
$<\mu>$	0.90	2.0	0.24	14
$<\mu_1>$	0.82	2.0	0.16	14
$<\mu_2>$	0.084	0.063	0.084	0.074
$<T_{min}>$ /a	69	82	33	132

Since the true semimajor axis $a = \rho r_E$ is not yielded by the fit, T is estimated using $\rho = \chi$, which corresponds to a minimal value T_{min}, because $\rho \geq \chi$ for any gravitationally bound system and $T \propto \rho^{3/2}$.

The distribution of the physical quantities as well as symmetric intervals around the expectation value with probabilities of 68.3 % and 95.4 % are shown in the previous section.

The model BA3 has previously been omitted (Dominik & Hirshfeld 1996) due to the fact that the mass ratio between the lens objects is very extreme ($4 \cdot 10^{-23}$), which corresponds to unphysical values (see Table 7). However, the uncertainty of the mass ratio is very large for extreme mass ratios (Dominik

Table 6. Expectation values for the point-source-point-mass-lens events towards the LMC. M # denotes MACHO events, while E # denotes EROS events.

	M #4	M #5	M #6	M #7	M #8	M #10	E #1	E #2
t_E/d	23	41	44	58	31	21	27	30
$<r_E>$ /AU	2.5	4.4	4.7	6.2	3.3	2.2	2.9	3.2
$<\mu>$	0.14	0.46	0.52	0.91	0.26	0.12	0.20	0.24

Table 7. Expectation values of the physical parameters and used fit parameters for the 6 binary lens models for MACHO LMC#1, denoted by BL, BL1, BA, BA1, BA2, and BA3, and for MACHO LMC#9.

	BL	BL1	BA	BA1	BA2	BA3	LMC#9
t_E/d	16.27	17.53	685	155	35.7	$2.62 \cdot 10^{12}$	143.4
$t_E^{(2)}/d$	—	—	17.57	15.15	17.72	16.36	—
m_1	0.463	0.557	0.99934	0.9904	0.75	$1 - 4 \cdot 10^{-23}$	0.620
r	1.16	0.795	$6.6 \cdot 10^{-4}$	$9.7 \cdot 10^{-3}$	0.33	$3.9 \cdot 10^{-23}$	0.613
χ	0.20	0.22	2.41	2.21	1.82	2.24	0.83
$\chi^{(1)}$	—	—	2.41	2.22	2.10	2.24	—
$<r_E>$ /AU	1.75	1.88	73.6	16.7	3.84	$2.82 \cdot 10^{11}$	15.3
$<r_E^{(2)}>$ /AU	—	—	1.89	1.63	1.90	1.76	—
$<2r_{hd}>$ /AU	0.71	0.82	355	73.6	14.0	$1.2 \cdot 10^{12}$	2.54
$<\mu>$	0.072	0.083	127	6.5	0.34	$1.9 \cdot 10^{21}$	5.6
$<\mu_1>$	0.033	0.046	127	6.4	0.26	$1.9 \cdot 10^{21}$	3.5
$<\mu_2>$	0.038	0.037	0.084	0.062	0.086	0.073	2.1
$<T_{min}>$ /a	0.98	1.1	257	107	39	$1.43 \cdot 10^7$	24

& Hirshfeld 1996) due to the fact that the lens behaves nearly like a Chang-Refsdal lens. The same degeneracy has recently been rediscovered in the context of lensing by a star with a planet by Gaudi & Gould (1997). Table 8 shows the estimates for the 4 wide binary lens models (BA, BA1, BA2, BA3) where fit parameters at the upper 2-σ-bounds of the mass ratio r have been used. It can be seen that the expectation values for the separation and the mass change dramatically for the fits with small values of r, leaving much room for speculations about the nature of the lens object.

Recently, Rhie & Bennett (1996) have speculated about a planetary companion in the MACHO LMC#1 event. However, as shown in this and the last section, there are two fundamental uncertainties (beyond the fact that there are only a few data points near the peak, which could have been solved by a denser sampling), namely the uncertainty in the mass ratio and the uncertainty due to the unknown lens position and its velocity. The planetary model of Rhie & Bennett (1996) corresponds to my model BA1, where the expectation value of the mass of the low-mass object is about $0.06\ M_\odot$. Taking into account an uncertainty of a factor of 30, a value of 2 Jupiter masses is reached just at the 2-σ-bound. As shown in Table 7, the expectation value for the mass of the low-mass object is about the same

for all of my wide binary lens fits, so that there are the same prospects for a planet as the low-mass object for all of these models. However, the high-mass object will be different.

The estimates of physical quantities like the mass of the lens object(s), their separation and the rotation periods along with the uncertainties involved are needed to reveal the physical nature of the lens for each observed event. One can check whether the mass range is consistent with the assumption of a dark object, and of which nature the lens should be in this case (brown dwarf, white dwarf, neutron star, ...). The determination of the mass range is crucial for claiming the existence of a planetary companion.

One can also check whether it is consistent to use a static binary lens model rather than one with rotating binary lens (Dominik 1997). Moreover, by comparing estimates for different lens populations (e.g. the galactic halo and the LMC halo) one may obtain indications to which population the lens belongs.

In contrast to estimates on the mass spectrum, there is no direct influence from the ensemble of observed events on the estimates for a specific event. However, there is an indirect influence, since the ensemble of events gives information about the mass spectrum, which in turn can be used to get a more accurate estimate for each observed event. However, a lot of

events (~ 100) are needed to get accurate information on the mass spectrum (Mao & Paczyński 1996). To be used for the estimates for a specific event, some of the higher mass moments should have been determined. Note that there will remain large uncertainties in the mass of a specific event even if the mass spectrum is known (unless it contains a sharp peak), since due to the broad distribution of the velocity, the range of timescales t_E for a certain mass is broad, so that the mass range for a specific event in turn may also be large.

While a white dwarf scenario is preferred by the LMC observations (e.g. Pratt et al. 1996), a brown-dwarf scenario is not ruled out (Spiro 1997) if one considers a flat halo. Though there are some restrictions on the average lens mass from the observed events, which will improve with more data, it will remain highly uncertain into which mass regime a certain event falls.

Since the ongoing microlensing observations constrain the galactic models and therefore give rise to more accurate determinations of the structure of the lens populations, the knowledge on specific events will also be improved by this.

References

Alcock C., Akerlof C. W., Allsman R. A., et al., 1993, Nat 365, 621

Alcock C., Allsman R. A., Axelrod T. S., et al., 1996, ApJ 461, 84

Alcock C., Allsman R. A., Alves D., et al., 1997, ApJ 486, 697

Ansari R., Cavalier F., Couchot F., et al., 1995, A&A 299, L21

Aubourg E., Bareyre P., Bréhin S., et al., 1993, Nat 365, 623

Beaulieu J. P., Ferlet R., Grison P., et al., 1995, A&A 299, 168

Bennett D. P., Alcock C., Allsman R. A., et al., 1996, Nucl. Phys. Proc. Suppl. 51, 152

Dominik M., 1996, Galactic microlensing beyond the standard model, PhD thesis, Universität Dortmund

Dominik M., 1997, Galactic microlensing with rotating binaries, preprint astro-ph/9702039, accepted for publication in A&A

Dominik M., Hirshfeld A.C., 1994, A&A 289, L31

Dominik M., Hirshfeld A.C., 1996, A&A 313, 841

Gaudi B. S., Gould A., 1997, ApJ 486, 85

Griest K., 1991, ApJ 366, 412

Jetzer Ph., 1994, ApJ 432, L43 (Erratum: 1995, ApJ 438, L49)

Jetzer Ph., Massó E., 1994, Phys. Lett. B 323, 347

Mao S., Paczyński B., 1991, ApJ 374, L37

Mao S., Paczyński B., 1996, ApJ 473, 57

Paczyński B., 1986, ApJ 304, 1

Paczyński B., 1996, ARA&A 34, 419

Pratt M. R., Alcock C., Allsman R. A., et al., 1996b, Nucl. Phys. Proc. Suppl. 51, 131

De Rújula A., Jetzer Ph., Massó E., 1991, MNRAS 250, 348

Rhie S. H., Bennett D. P., 1996, Nucl. Phys. Proc. Suppl. 51, 86

Spiro M., 1997, Proceedings of the 3rd International Worskhop on Gravitational Microlensing Surveys, Notre Dame, IN, USA

Stubbs C., et al. (MACHO collaboration), 1997, http://darkstar.astro.washington.edu
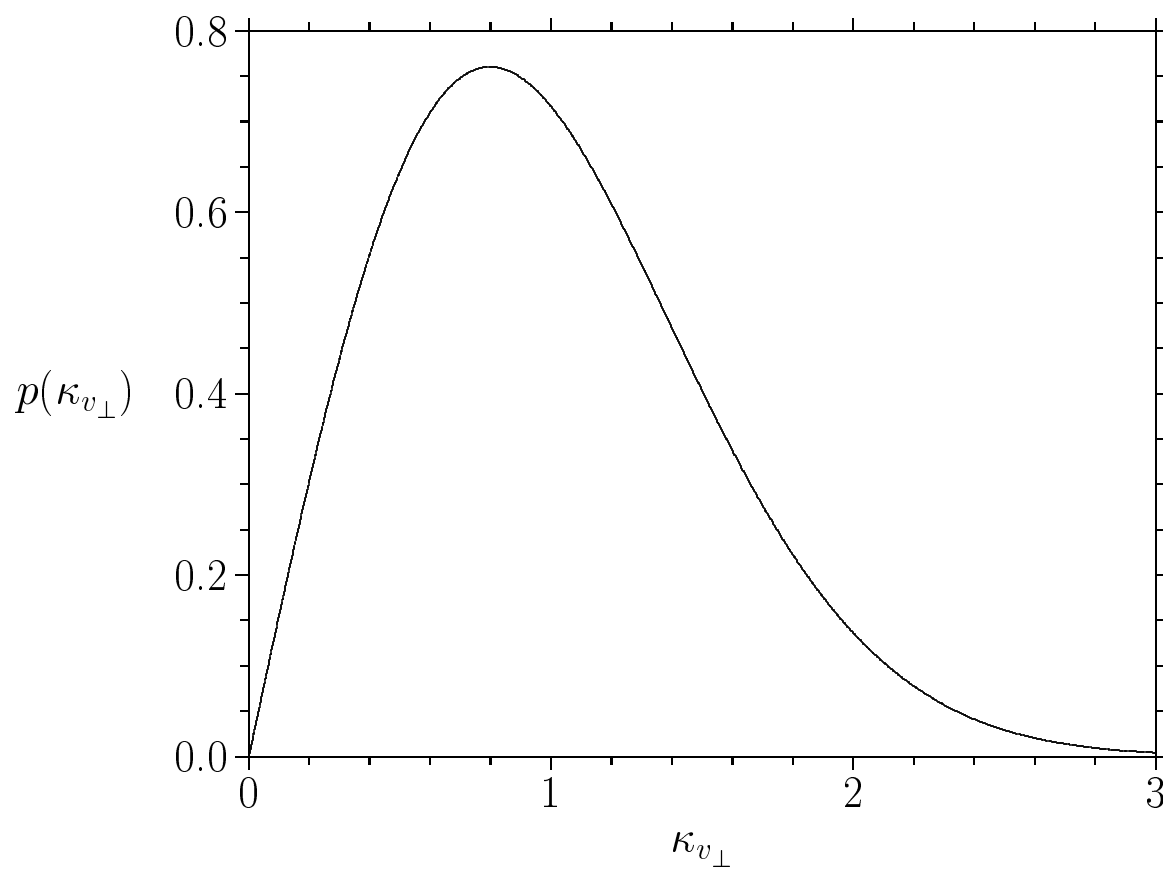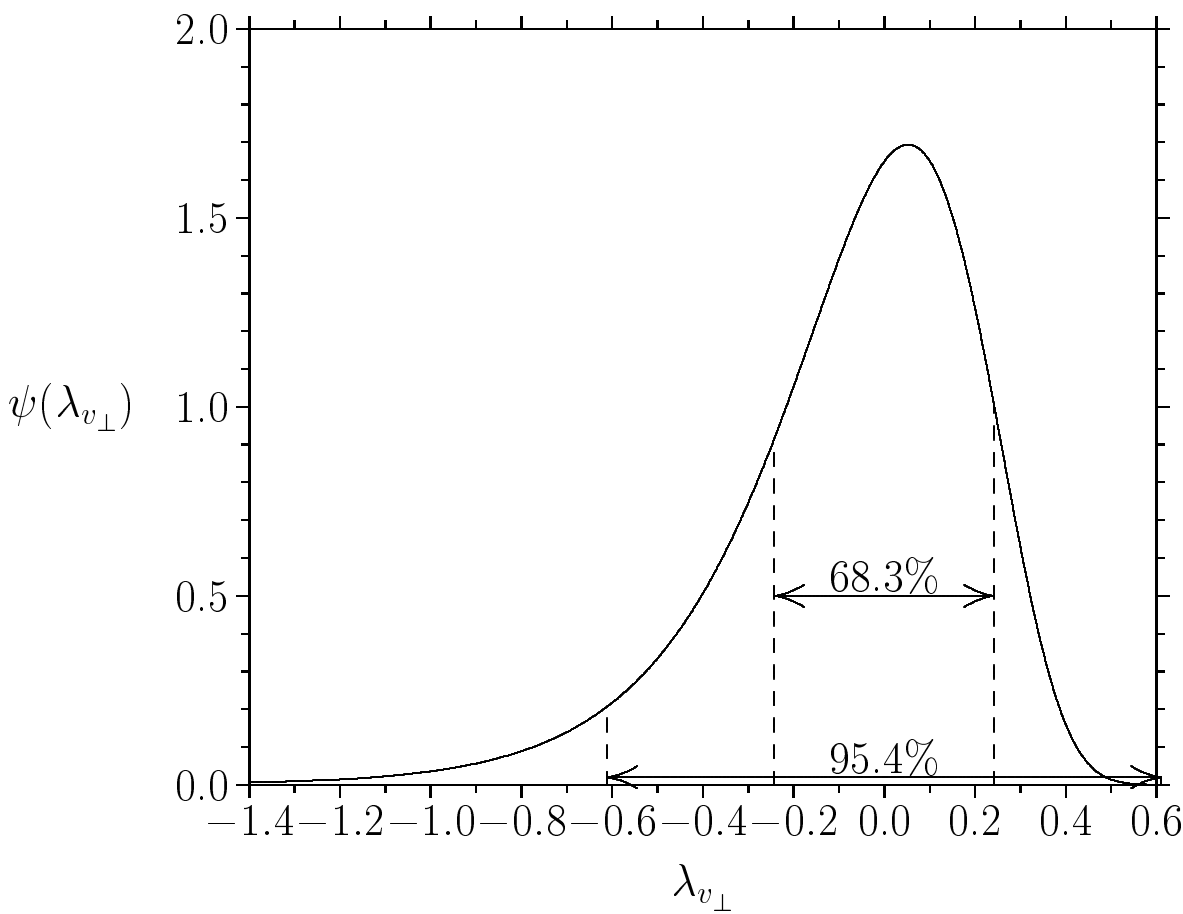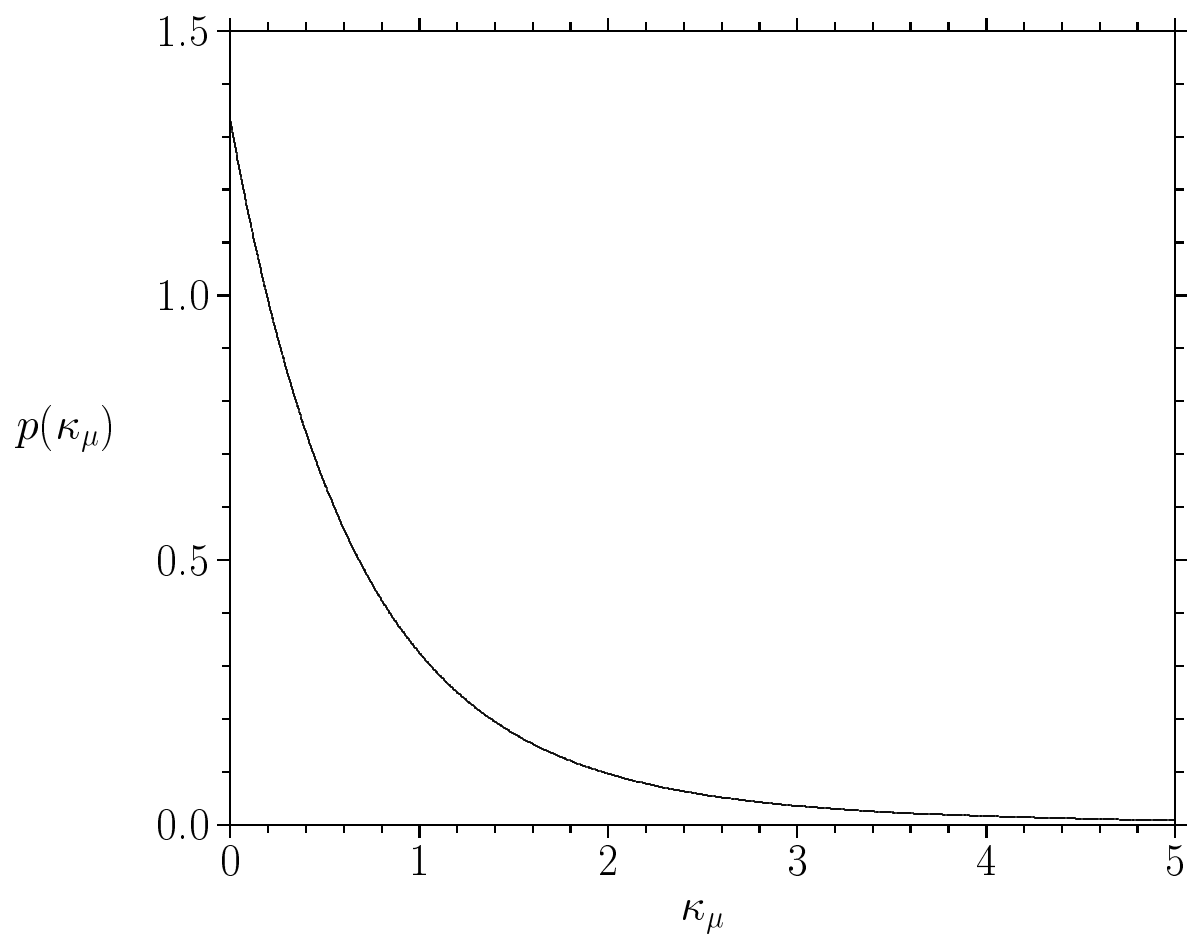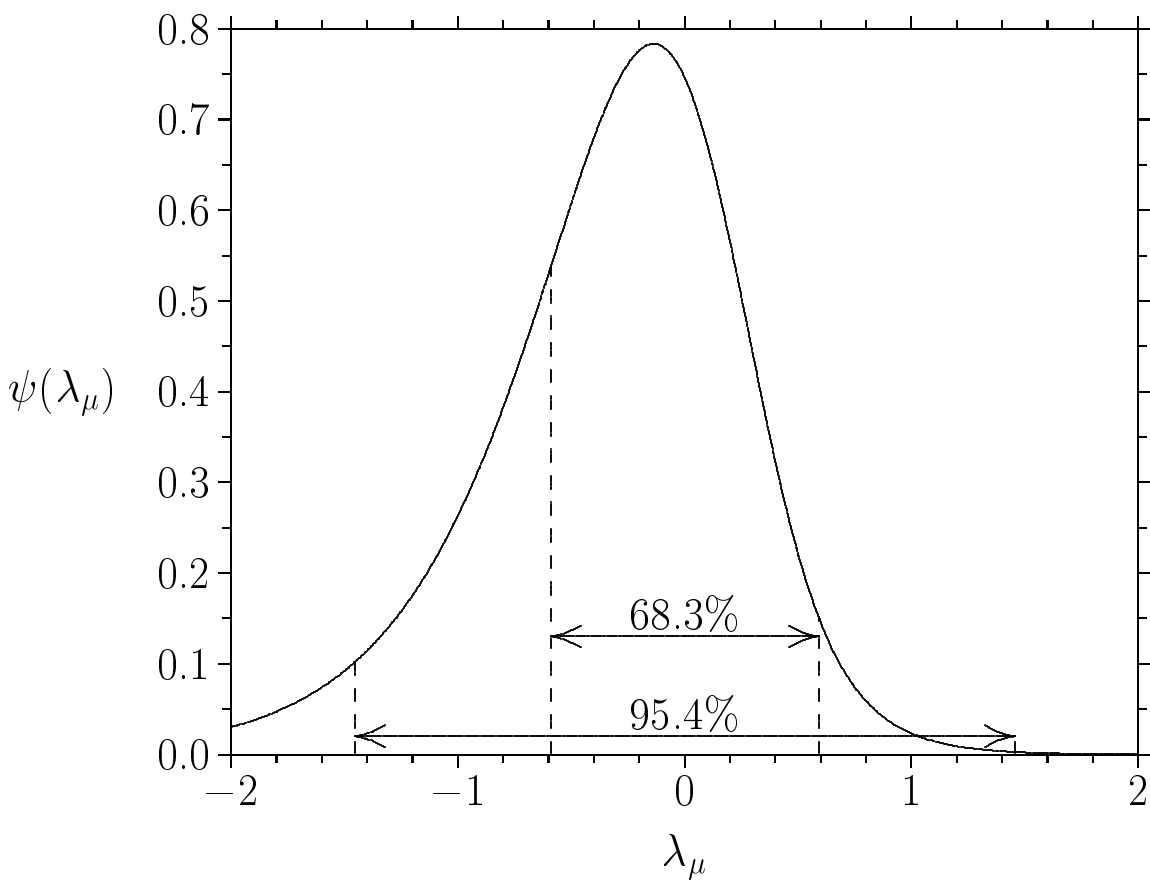
Figure 1 (left)

Figure 1 (right)
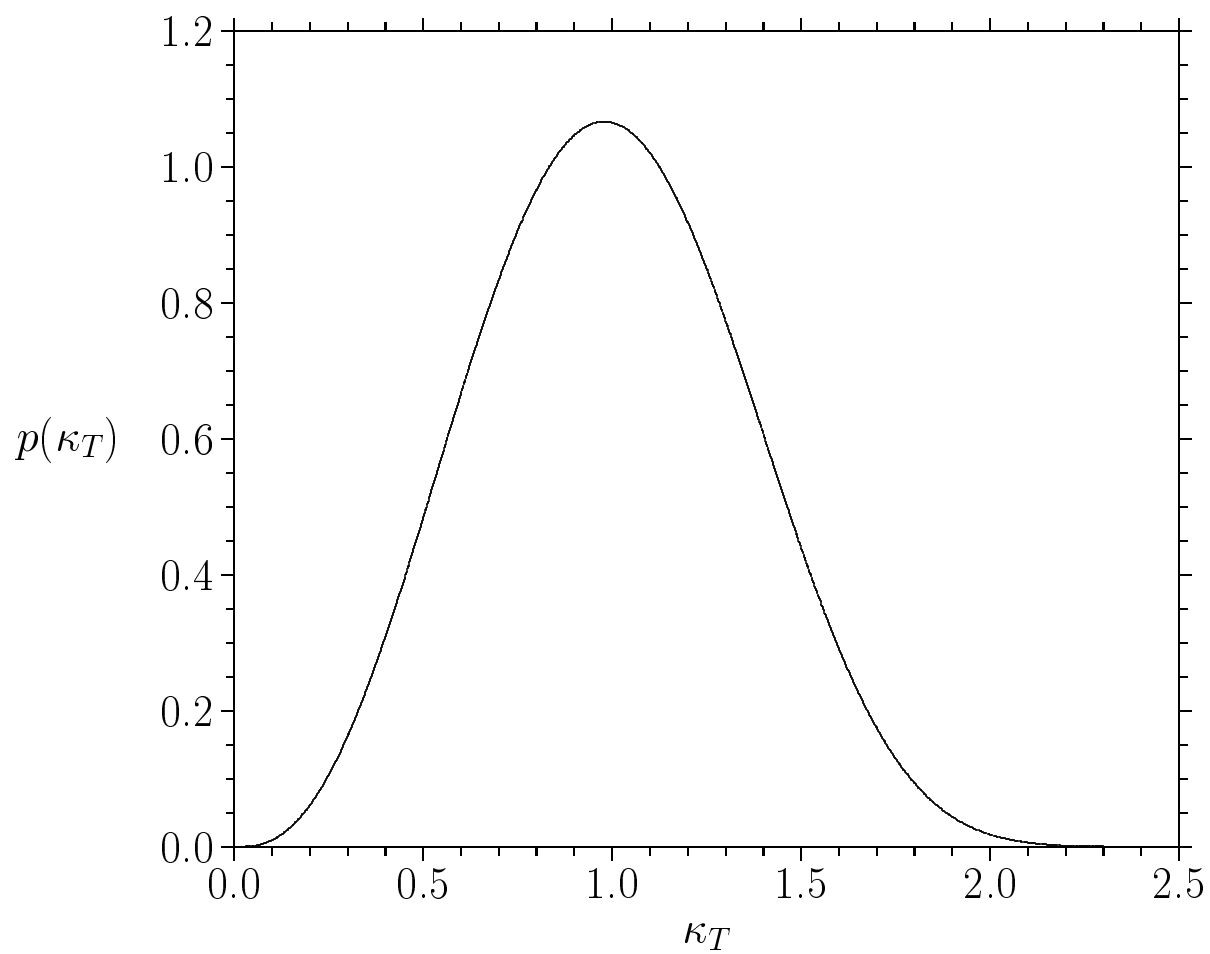
Figure 2 (left)

Figure 2 (right)

Figure 3 (left)

Figure 3 (right)